Pharmacol : 18–21, 2007
5) Delgado PL, Price LH, Miller HL et al : Serotonin and the neurobiology of depression. Effects of tryptophan depletion in drug-free depressed patients. Arch Gen Psychiatry 51 : 865–874, 1994
6) Egan MF, Kojima M, Callicott JH et al : The BDNF val66met polymorphism affects activity-dependent secretion of BDNF and human memory and hippocampal function. Cell 112 : 257–269, 2003
7) Eley TC, Sugden K, Corsico A et al : Gene-environment interaction analysis of serotonin system markers with adolescent depression. Mol Psychiatry 9 : 908–915, 2004
8) Federenko IS, Nagamine M, Hellhammer DH et al : The heritability of hypothalamus pituitary adrenal axis responses to psychosocial stress is context dependent. J Clin Endocrinol Metab 89 : 6244–6250, 2004
9) Francis D, Diorio J, Liu D et al : Nongenomic transmission across generations of maternal behavior and stress responses in the rat. Science 286 : 1155–1158, 1999
10) Gillespie NA, Whitfield JB, Williams B et al : The relationship between stressful life events, the serotonin transporter (5-HTTLPR) genotype and major depression. Psychol Med 35 : 101–111, 2005
11) Gotlib IH, Joormann J, Minor KL et al : HPA Axis Reactivity: A Mechanism Underlying the Associations Among 5-HTTLPR, Stress, and Depression. Biol Psychiatry, 2007
12) Groves JO : Is it time to reassess the BDNF hypothesis of depression? Mol Psychiatry 12 : 1079–1088, 2007
13) Heim C, Mletzko T, Purselle D et al : The Dexamethasone/Corticotropin-Releasing Factor Test in Men with Major Depression: Role of Childhood Trauma. Biol Psychiatry, 2007
14) Heim C, Newport DJ, Heit S et al : Pituitary-adrenal and autonomic responses to stress in women after sexual and physical abuse in childhood. JAMA 284 : 592–597, 2000
15) Hu XZ, Lipsky RH, Zhu G et al : Serotonin transporter promoter gain-of-function genotypes are linked to obsessive-compulsive disorder. Am J Hum Genet 78 : 815-826, 2006
16) Kim JM, Stewart R, Kim SW et al : Interactions between life stressors and susceptibility genes (5-HTTLPR and BDNF) on depression in Korean elders. Biol Psychiatry 62 : 423–428, 2007
17) Krishnan V, Han MH, Graham DL et al : Molecular adaptations underlying susceptibility and resistance to social defeat in brain reward regions. Cell 131 : 391–404, 2007
18) Kunugi H, Ida I, Owashi T et al : Assessment of the dexamethasone/CRH test as a state-dependent marker for hypothalamic-pituitary-adrenal (HPA) axis abnormalities in major depressive episode: a Multicenter Study. Neuropsychopharmacology 31 : 212–220, 2006
19) Lesch KP, Bengel D, Heils A et al : Association of anxiety-related traits with a polymorphism in the serotonin transporter gene regulatory region. Science 274 : 1527–1531, 1996
20) Maciejewski PK, Prigerson HG, Mazure CM : Sex differences in event-related risk for major depression. Psychol Med 31 : 593–604, 2001
21) Mandelli L, Serretti A, Marino E et al : Interaction between serotonin transporter gene, catechol-O-methyltransferase gene and stressful life events in mood disorders. Int J Neuropsychopharmacol 10 : 437–447, 2007
22) McGuffin P, Rijsdijk F, Andrew M et al : The heritability of bipolar affective disorder and the genetic relationship to unipolar depression. Arch Gen Psychiatry 60 : 497–502, 2003
23) Miller CA, Sweatt JD : Covalent modification of DNA regulates memory formation. Neuron 53 : 857–869, 2007
24) Miller HL, Delgado PL, Salomon RM et al : Clinical and biochemical effects of catecholamine depletion on antidepressant-induced remission of depression. Arch Gen Psychiatry 53 : 117–128, 1996
25) Modell S, Lauer CJ, Schreiber W et al : Hormonal response pattern in the combined DEX-CRH test is stable over time in subjects at high familial risk for affective disorders. Neuropsychopharmacology 18 : 253–262, 1998
26) Moreno FA, Rowe DC, Kaiser B et al : Association between a serotonin transporter promoter region polymorphism and mood response during tryptophan depletion. Mol Psychiatry 7 : 213–216, 2002
27) Neumeister A, Konstantinidis A, Stastny J et al : Association between serotonin transporter gene promoter polymorphism (5HTTLPR) and behavioral responses to tryptophan depletion in healthy women with and without family history of depression. Arch Gen Psychiatry 59 : 613–620, 2002
28) Neumeister A, Turner EH, Matthews JR et al :

Effects of tryptophan depletion vs catecholamine depletion in patients with seasonal affective disorder in remission with light therapy. Arch Gen Psychiatry 55 : 524–530, 1998
29) Piccinelli M, Wilkinson G : Gender differences in depression. Critical review. Br J Psychiatry 177 : 486–492, 2000
30) Pizarro JM, Lumley LA, Medina W et al : Acute social defeat reduces neurotrophin expression in brain cortical and subcortical areas in mice. Brain Res 1025 : 10–20, 2004
31) Salomon RM, Miller HL, Krystal JH et al : Lack of behavioral effects of monoamine depletion in healthy subjects. Biol Psychiatry 41 : 58–64, 1997
32) Schule C, Zill P, Baghai TC et al : Brain-derived neurotrophic factor Val66Met polymorphism and dexamethasone/CRH test results in depressed patients. Psychoneuroendocrinology 31 : 1019–1025, 2006
33) Shirayama Y, Chen AC, Nakagawa S et al : Brain-derived neurotrophic factor produces antidepressant effects in behavioral models of depression. J Neurosci 22 : 3251–3261, 2002
34) Silberg J, Pickles A, Rutter M et al : The influence of genetic factors and life stress on depression among adolescent girls. Arch Gen Psychiatry 56 : 225–232, 1999
35) Smith J, Prior M : Temperament and stress resilience in school-age children: a within-families study. J Am Acad Child Adolesc Psychiatry 34 : 168–179, 1995
36) Sullivan PF, Kendler KS, Neale M : Schizophrenia as a complex trait: evidence from a meta-analysis of twin studies. Arch Gen Psychiatry 60 : 1187–1192, 2003
37) Sullivan PF, Neale MC, Kendler KS : Genetic epidemiology of major depression: review and meta-analysis. Am J Psychiatry 157 : 1552–1562, 2000
38) Surtees PG, Wainwright NW, Willis-Owen SA et al : Social adversity, the serotonin transporter (5-HTTLPR) polymorphism and major depressive disorder. Biol Psychiatry 59 : 224–229, 2006
39) Uher R, McGuffin P : The moderation by the serotonin transporter gene of environmental adversity in the aetiology of mental illness: review and methodological analysis. Mol Psychiatry, 2007
40) Videbech P, Ravnkilde B : Hippocampal volume and depression: a meta-analysis of MRI studies. Am J Psychiatry 161 : 1957–1966, 2004
41) Weaver IC, Cervoni N, Champagne FA et al : Epigenetic programming by maternal behavior. Nat Neurosci 7 : 847–854, 2004

* * *

⊙シリーズ 精神医学用語解説 ********** Psychiatric Technical Term

341. 手綱核

［英］habenula

解剖学的構造と機能

手綱核(habenula)とは，間脳の最背側部に両側性に存在し，終脳と髄条によって結ばれ，その状態が手綱のようであるから手綱核と名付けられた。その全体の構造を，手綱核構造体(habenular complex)と総称する場合もある。長らくその解剖学的構造と機能は不明だったが，最近約20年間のラットやネコにおける研究により，明らかになってきた[8]。基本的には，上行性のモノアミン神経系およびアセチルコリン神経系の制御を行い，終脳(hindbrain)，中脳(midbrain)，前脳(forebrain)を結ぶ重要な神経回路を構成すると考えられている[8]。解剖学的に詳細に記述すると，両側性に存在する大脳の情動系神経核群(いわゆる大脳辺縁系の一部を含む)と，中脳と後脳の境界部に接する腹側正中線上に存在する中脳脚間核を中継する神経回路を構成しているとされる[8]。

進化学的にも重要な解剖学的構造であることは，本神経回路が魚類からヒトまで共通して存在するによっても示されている[1,2]。

哺乳類では，手綱核は内側核と外側核の独立した二つの構造体によって構成され，前者は，さらに5つ，後者は10の核構造体に下位分類されている[4,7]。内側核および外側核は，それぞれ異なった機能的役割を持つと報告されている[8]。

内側手綱核には，外界の物理的状況とその情動的価値の情報が，海馬と扁桃体から，中隔核と分界線条核を介して伝わるとされ，左右の内側手綱核は，反屈束に沿って伸びる神経によって，脚間核とつながっている。脚間核は，さらに腹側被蓋野のドーパミン神経細胞や，縫線核のセロトニン神経細胞などのモノアミン神経細胞の活動を制御していると考えられている[8]。

外側手綱核には，選択された行動プログラムに関わる大脳皮質・基底核・視床ループの細胞集団の興奮に関する情報が，腹側淡蒼球から運ばれる。外側手綱核から伸びる神経は，脚間核を介さずに直接に，腹側被蓋野や縫線核に投射しモノアミン神経系を制御していると考えられている[8]。

上記のような神経回路の特徴から，手綱核においては，外界の物理的情報とその情動的価値を背景とした行動プログラムの選択に関わる入力情報と出力情報が集積されるため，手綱核は状況にふさわしい行動プログラムが選択されているかどうかを検証するメカニズムに関与しているのではないかとする仮説がたてられている[1,2]。つまり，価値判断を伴った外界状況に関する情報(外部環境情報)と，それによって喚起された目的を持った行動に関する情報(内部行動プログラム情報)との照合が行われ，その照合が一致しないときに，モノアミン作動性神経細胞の活性の調節によって，行動プログラムのための大脳皮質・基底核・視床ループの神経回路の制御が行われるというものである[1,2]。

最近の報告では，ヒトにおいて，スクリーンに映る異なる速度でゴールに向かう2つのボールのどちらが先にゴールに達するかを被験者に予言させた場合，被験者が間違った解答をしたと知らされた場合に，手綱核の活動が選択的に亢進することが報告されている[12]。また，サルにおいては，報酬を期待し，その報酬が得られなかった場合に，外側手綱核の興奮が高まることが，最近報告されている[9]。

手綱核と精神疾患

手綱核は，その特異的神経結合から，さまざまな精神疾患との関連が指摘されている。

1) "うつ病"との関係

慢性的に軽度のストレス下に置かれたラットは，強制水泳条件下において，脱出行動を取らずに無動作となり，学習性無力状態に陥る。背側縫線核神経細胞からセロトニン分泌が低下しており，外側手綱核破壊によって，セロトニン分泌の低下や，学習性無力状態が抑制されることが報告されている[3,8,11]。

2)薬物依存症との関係

ラットでは，ニコチンやアンフェタミンの過剰摂取は，それぞれ内側手綱核と外側手綱核に特異的的障害を及ぼすことが知られており，ヒトにおいても，薬物依存との関係が示唆されている[5,6]。

3)統合失調症との関係

統合失調症の患者で，手綱核が石灰化している頻度が有意に高いという報告[6]や，ラットにおいてアンフェタミンやコカイン依存を起こすと特異的に手綱核が委縮するとの報告もある[10]。

文献

1) Aizawa H, Bianco IH, Hamaoka T et al : Laterotopic representation of left-right information onto the dorso-ventral axis of a zebrafish midbrain target nucleus. Curr Biol 15 : 238–243, 2005
2) Aizawa H, Goto M, Sato T et al : Temporally regulated asymmetric neurogenesis causes left-right difference in the zebrafish habenular structures. Dev Cell 12 : 87–98, 2007
3) Amat J, Sparks PD, Matus-Amat P et al : The role of the habenular complex in the elevation of dorsal raphe nucleus serotonin and the changes in the behavioral responses produced by uncontrollable stress. Brain Res 917 : 118–126, 2001
4) Andres KH, von During M, Veh RW : Subnuclear organization of the rat habenular complexes. J Comp Neurol 407 : 130–150, 1999
5) Carlson J, Noguchi K, Ellison G : Nicotine produces selective degeneration in the medial habenula and fasciculus retroflexus. Brain Res 906 : 127–134, 2001
6) Ellison G : Stimulant-induced psychosis, the dopamine theory of schizophrenia, and the habenula. Brain Res Brain Res Rev 19 : 223–239, 1994
7) Geisler S, Andres KH, Veh RW : Morphologic and cytochemical criteria for the identification and delineation of individual subnuclei within the lateral habenular complex of the rat. J Comp Neurol 458 : 78–97, 2003
8) Lecourtier L, Kelly PH : A conductor hidden in the orchestra? Role of the habenular complex in monoamine transmission and cognition. Neurosci Biobehav Rev 31 : 658–672, 2007
9) Matsumoto M, Hikosaka O : Negative motivational control of saccadic eye movement by the lateral habenula. Prog Brain Res 171 : 399–402, 2008
10) Sandyk R : Pineal and habenula calcification in schizophrenia. Int J Neurosci 67 : 19–30, 1992
11) Sartorius A, Henn FA : Deep brain stimulation of the lateral habenula in treatment resistant major depression. Med Hypotheses 69 : 1305–1308, 2007
12) Ullsperger M, von Cramon DY : Error monitoring using external feedback: specific roles of the habenular complex, the reward system, and the cingulate motor area revealed by functional magnetic resonance imaging. J Neurosci 23 : 4308–4314, 2003

川嵜弘詔，小林祐樹，神庭重信
(九州大学大学院医学研究院精神病態医学分野)

*　　*　　*

Brief Communications

Abnormal Neural Oscillatory Activity to Speech Sounds in Schizophrenia: A Magnetoencephalography Study

Shogo Hirano, Yoji Hirano, Toshihiko Maekawa, Choji Obayashi, Naoya Oribe, Toshihide Kuroki, Shigenobu Kanba, and Toshiaki Onitsuka

Department of Neuropsychiatry, Graduate School of Medical Sciences, Kyushu University, Fukuoka 812-8582, Japan

Schizophrenia impairs many cognitive functions, and abnormalities in language processing have been proposed as one of the bases for this disorder. Previously, it was reported that different magnetoencephalography (MEG) patterns of the evoked oscillatory activity (eOA) of 20–45 Hz to speech and nonspeech sounds were evidence of a fast mechanism for the representation and identification of speech sounds in humans. The current study tested the hypothesis that the schizophrenics would show abnormal neural oscillatory activity, as measured by eOA, to speech and nonspeech sounds. Twenty patients and 23 control subjects participated in this study. MEG responses to speech and nonspeech sounds were recorded and eOA power and phase locking at 20–45 Hz were analyzed. Patients showed significantly delayed peak latencies of the eOA power and phase locking to speech sounds in the left hemisphere and to nonspeech sounds in the right hemisphere. Patients also showed a significantly reduced eOA power to speech sounds in the left hemisphere in 0–50 ms and a significantly larger eOA power to speech sounds in the left hemisphere in 100–150 ms. In addition, the analyses of the lateralization index revealed the pattern of hemispheric lateralization to be the opposite in patients. These results indicated that patients showed different characteristics of eOA compared with normal controls, probably related to deficits in a fast mechanism for identifying speech sounds. Moreover, the present study suggests that schizophrenia might be characterized by an opposite pattern of hemispheric lateralization in auditory evoked oscillations.

Key words: evoked oscillatory activity; schizophrenia; speech sounds; magnetoencephalography; lateralization; wavelet transform

Introduction

Speech sound recognition may be qualitatively different from other recognition systems in terms of the underlying neurobiological structure and developmental trajectory. Belin et al. (2000) reported that human voices were perceived, at least in part, by a processing stream separate from that used in processing other nonvocal environmental sounds. From an evolutionary perspective, speech sound recognition represents a significant element of verbal decoding to solve adaptive problems critical for survival. Accordingly, the human brain must have a fast mechanism for representing and identifying speech sounds.

The neural oscillatory activity in high-frequency, in particular, in the gamma (30–80 Hz) and beta (15–30 Hz) bands, is supposed to play a critical role in feature binding and object representation (Uhlhaas and Singer, 2006). The functional roles of the evoked and induced oscillatory activity have been specifically investigated in humans (Uhlhaas and Singer, 2006). The evoked oscillatory activity (eOA) is phase locked to the onset of stimuli. Herrmann et al. (2004) suggested that the eOA occurring within 150 ms after stimulation reflected the rapid matching of bottom-up signals with memory contents.

In schizophrenia, abnormal eOA has been repeatedly reported in auditory and visual perception processes. In the auditory gamma band eOA, Kwon et al. (1999) reported reduced 40 Hz steady-state eOA in schizophrenia. Hong et al. (2004) showed reduced steady-state eOA at 40 Hz in first-degree relatives with schizophrenia spectrum personality symptoms. For visual perception, Spencer et al. (2003, 2004) demonstrated that visual gestalt stimuli lead to abnormal eOA at ~40 Hz over the occipital lobe in schizophrenia, and that this abnormal eOA was associated with visual hallucinations. In the beta band, Uhlhaas et al. (2006) reported that the deficits in Gestalt perception in schizophrenia were associated with reduced phase-synchrony of eOA.

Magnetoencephalography (MEG) offers millisecond resolution to detect neuronal activity to auditory stimuli. Palva et al. (2002) reported different MEG patterns of the eOA within 100 ms after stimulation to speech and nonspeech sounds in healthy subjects. They interpreted that different MEG patterns of the eOA at 20–45 Hz between speech and nonspeech sounds indicated the existence of a fast mechanism for representing and identifying speech sounds in the human auditory cortex.

Schizophrenia is characterized by positive symptoms (e.g., hallucination, delusion), negative symptoms (e.g., affective flattening, anhedonia), and disorganization of thought perhaps re-

Received June 14, 2007; revised March 21, 2008; accepted March 21, 2008.

This work was supported in part by a grant from Research Group For Schizophrenia, Japan (T.O.), Grants-in-Aid for Scientific Research C17591218 (T.O.) and B19390306 (S.K.) from the Ministry of Education, Culture, Sports, Science, and Technology, Japan, and Grant H18 kokoro-ippan-012 from Ministry of Health, Labor and Welfare, Japan (S.K.). Our appreciation is expressed to Drs. Takefumi Ueno, Takehito Hayami, and Seiichi Sakatani for clarification regarding methodology. We gratefully acknowledge the technical support of Yuko Somehara.

Correspondence should be addressed to Dr. Toshiaki Onitsuka, Department of Neuropsychiatry, Graduate School of Medical Sciences, Kyushu University, 3-1-1, Maidashi, Higashiku, Fukuoka 812-8582, Japan. E-mail: toshiaki@npsych.med.kyushu-u.ac.jp.

DOI:10.1523/JNEUROSCI.5031-07.2008

 0270-6474/08/284897-07$15.00/0

lated to abnormal language processing. Several studies investigated the eOA at ~40 Hz to auditory "nonspeech" sounds in schizophrenia (Haig et al., 2000; Gallinat et al., 2004). However, it would be important to investigate MEG patterns of the early eOA to speech sounds in schizophrenia, because auditory verbal hallucinations are often shown in schizophrenia and abnormalities in language processing have been proposed as one of the bases for schizophrenia (Nestor et al., 2001).

The present study was designed to test the hypothesis that the schizophrenics will show abnormal early neural oscillatory activity to speech sounds, as measured by the eOA at 20–45 Hz within 150 ms after stimulation, and that this abnormal eOA will be associated with the severity of auditory hallucinations.

Table 1. Demographic and clinical characteristics of the study groups

	Schizophrenia	Normal controls	df	t or χ^2	p
Sex (male/female)	15/5	13/10	1	1.61	0.21
Age (years)	35.3 ± 12.2	33.6 ± 6.7	41	−0.55	0.59
Handedness	98.3 ± 4.1	97.8 ± 6.4	41	−0.26	0.92
SES[a]	3.45 ± 0.94	1.78 ± 0.90	41	−5.91	<0.001
Parental SES	2.15 ± 0.67	2.52 ± 0.90	41	1.52	0.14
Medication dose (CPZ equivalent; mg)	550 ± 325				
Symptom onset (years)	22.4 ± 5.3				
Duration of illness (years)	12.9 ± 10.7				
SAPS global ratings					
Hallucinations	2.9 ± 1.7				
Delusions	2.8 ± 1.7				
Bizarre behavior	2.7 ± 1.3				
Thought disorder	2.9 ± 1.4				
SANS global ratings					
Affective flattening	3.0 ± 1.3				
Alogia	2.6 ± 1.2				
Avolition	2.7 ± 1.2				
Anhedonia	2.7 ± 1.2				
Inattention	3.2 ± 1.1				

CPZ, Chlorpromazine.

[a]Patients with schizophrenia showed a significantly lower SES than normal controls.

Materials and Methods

Subjects. Twenty patients (15 males) and 23 normal control subjects (13 males) with normal hearing (age 18–57, all right handed) participated in this study. After a complete description of the study, all participants signed an informed consent form according to the regulations of the Ethics Commission of the Graduate School of Medical Sciences, Kyushu University. Demographic data for all subjects are presented in Table 1. The exclusion criteria were as follows: (1) neurologic illness or major head trauma that would result in abnormal electroencephalography (EEG); (2) electroconvulsive therapy; (3) alcohol or drug dependence; (4) alcohol or drug abuse within the past five years; or (5) a verbal intelligence quotient <75. Normal controls were screened using the Structured Clinical Interview (SCID), nonpatient edition. No normal controls had an Axis I psychiatric disorder in themselves or their first-degree relatives.

All patients were recruited from Kyushu University Hospital and were diagnosed to have schizophrenia based on the SCID for the *Diagnostic and Statistical Manual of Mental Disorders*, edition IV, and medical records. All patients were receiving neuroleptic medication, with a mean daily dose equivalent to 550 ± 325 mg of chlorpromazine [typical neuroleptics (1 of the 20 patients), atypical (9), or both (10)]. The Scale for the Assessment of Positive Symptoms (SAPS) and the Scale for the Assessment of Negative Symptoms (SANS) were administered to patients. Socioeconomic status (SES) of subjects and parental SES were measured using the Hollingshead two-factor index.

Stimulation and procedures. During the experiment, all subjects were in the lateral recumbent position on a bed in a magnetically shielded room at Kyushu University Hospital. Auditory evoked responses in both hemispheres were recorded alternately (left and right hemispheres counterbalanced between subjects). The subjects were instructed to keep their eyes open and not to sleep. A 2000 Hz steady-state pure tone was used as the auditory nonspeech stimulus, and the Japanese vowel sound /a/ was used as the auditory speech stimulus. The speech stimulus was the voice spoken by an actor who was a native Japanese speaker. The frequencies for the formants (F) of the vowel /a/ were as follows: F0 = 140 Hz, F1 = 760 Hz, F2 = 1250 Hz, F3 = 2750 Hz, and F4 = 3600 Hz. Both stimuli were edited with 200 ms duration (rise/fall time, 10 ms). At the earpiece, the intensity of each stimulus was the 60 dB sound pressure level.

Stimuli were delivered to the ear contralateral to the hemisphere being recorded through a 2.3 m plastic tube with a plastic insert earpiece at the tip. Both stimuli were presented in a pseudorandom order until the sum of the numbers of each stimulus was up to 440. The interstimulus intervals were between 1 and 2 s. The subjects were instructed to ignore the auditory stimuli.

Data acquisition and data analysis. A 37-channel biomagnetometer was used. The sampling frequency was 4167 Hz. The whole sweep time was 300 ms (from −50 to 250 ms after stimulation). Epochs with signal variations exceeding 4.0 pT were excluded. To extract eOA at 20–45 Hz, all of the epochs and the averaged epochs for each condition were applied to the continuous wavelet transform (CWT). CWT was performed using the Matlab Wavelet Toolbox. The complex Morlet wavelet was used as the mother wavelet: $W(t) = (\pi f_b)^{-0.5} \times \exp(-t^2/f_b^2) \times \exp(2i\pi f_c t)$. f_b is a bandwidth parameter, and f_c is a wavelet center frequency parameter. In this analysis, f_b and f_c were chosen to be 1. We used scales from 167 to 52 in the CWT, corresponding approximately to 20–45 Hz. We used the squared modulus of the result of CWT on the averaged epochs as the eOA power. The square-root transform was applied to the eOA power for normalization, and the mean eOA power of the prestimulus baseline (from −50 to 0 ms) was subtracted from the poststimulus eOA power for each frequency for baseline correction (Kiebel et al., 2005). The eOA power maps of the 10 channels with the largest power within 20–45 Hz and 0–150 ms were averaged to insure a reasonably high signal-to-noise ratio (Palva et al., 2002) (see Fig. 1*A*). We also calculated eOA phase-locking using the following formula: phase-locking$(t) = 1/N \times |\Sigma z(t)|$, where N is the number of epochs and $z(t)$ refers to the continuous phase of a single trial. Note that z is a complex value on the unit circle, i.e., $z = \exp(j\theta)$, where θ is the phase of an oscillation and j is the imaginary unit (Tallon-Baudry et al., 1996). We applied baseline correction to and averaged the eOA phase-locking across 10 channels in the same way and channels in the analyses of the eOA power. The eOA power and phase-locking peak latency was defined as the latency with the largest power and phase-locking averaged across 20–45 Hz within 0–150 ms. To investigate the eOA power change over time, we divided the eOA power maps at 20–45 Hz into three periods: 0–50 ms, 50–100 ms, and 100–150 ms, and averaged the eOA power across 20–45 Hz in each period (hereinafter called mean eOA power).

The positive wave elicited by auditory stimulation at around 50 ms has been defined as the P50, and the negative wave elicited at around 100 ms has been defined as the N100. P50m and N100m are the magnetic counterparts of P50 and N100, respectively. We also investigated the peak amplitudes and latencies of the P50m and the N100m in the filtered (1–20 Hz) conventional evoked responses. For each component, the peak root mean square (RMS) was computed with the following formula: $\mathrm{RMS}(t) = [\Sigma x(i,t)^2/n]^{0.5}$, where $x(i,t)$ is the magnetic field for each channel ($i = 1 - 10$) at time t and $\Sigma x(i,t)^2/10$ is the square mean of the magnetic field of the same 10 channels used in the analysis of the eOA power. The P50m latency was defined as the latency with the largest RMS between 20 and 70 ms. The N100m was also defined as between 80 and 120 ms. We also evaluated the lateralization index (LI) of the mean eOA power, the eOA power and phase-locking peak latency for each subject as

$(L - R)/(|L| + |R|)$, with L and R being the values in the left and right hemisphere (Kircher et al., 2004).

Statistical analysis. The mean eOA powers were submitted to a repeated-measures ANOVA (rmANOVA) with group as a between-subjects factor, and stimulus (speech or nonspeech), hemisphere (left or right), and period (three periods) as within-subjects factors. For the eOA power peak latency, phase-locking peak latency, the P50m, and the N100m, rmANOVAs were performed with group as a between-subjects factor, and stimulus and hemisphere as within-subjects factors. LI of these indices were submitted to the same rmANOVA without a hemisphere factor.

The associations between the clinical symptoms and the mean eOA powers to speech sounds in patients were investigated, where the increased severity of auditory hallucinations was predicted to be significantly associated with reduced eOA power. Correlations between auditory hallucinations and the mean eOA powers were evaluated using Spearman's rho.

Results

Demographics

There were no significant group differences in the age, handedness, or parental SES. Patients had significantly lower SES than normal controls ($t_{(41)}$=-5.91; $p < 0.001$), consistent with reduced functioning because of the disorder (Table 1). In addition, there was no significant correlation between the medication dose and eOA ($-0.22 \leq$ rho ≤ 0.43; $0.06 \leq p \leq 0.99$).

eOA power peak latency and eOA phase-locking peak latency

We show the topography of the magnetic field and of the spatial derivative at the eOA power peak latency and at the N100m in Figure 1*B*. Spatial derivative was computed with the following formula: spatial derivative $= |\nabla B(u,v)| = ((\partial B/\partial u)^2 + (\partial B/\partial v)^2)^{0.5}$, where $B(u,v)$ is measured axial magnetic field, and u and v are local coordinates (Bastiaansen and Knösche, 2000). Figure 1*C* shows the grand average eOA power maps. The eOA power maps show clear oscillatory activity at 20–45 Hz in both groups for each condition. Figure 1*D* shows the eOA power and phase-locking waveforms and the auditory evoked responses for each condition. The eOA power and phase-locking peak latencies and LI are shown in Figure 2.

In terms of the eOA power peak latency, an rmANOVA demonstrated a significant main effect of group ($F_{(1,41)} = 7.1$; $p = 0.01$) and hemisphere by stimulus by group ($F_{(1,41)} = 15.5$; $p < 0.001$) interaction, with no other significant main effects or interactions ($0.1 \leq F_{(1,41)} \leq 2.9$; $0.09 \leq p \leq 0.74$). To delineate this hemisphere by stimulus by group interaction, a follow-up rmANOVA was performed for each stimulus.

For speech sounds, the rmANOVA showed a significant main effect of group ($F_{(1,41)} = 4.8$; $p = 0.04$) and hemisphere by group interaction ($F_{(1,41)} = 14.0$; $p = 0.001$), with no main effect of hemisphere ($F_{(1,41)} = 0.6$; $p = 0.43$). To delineate this hemisphere by group interaction, the differences of the eOA power peak latency between the groups were investigated using *t* tests for each hemisphere. In the left hemisphere, patients showed significantly delayed eOA power peak latencies ($t_{(41)}$=-3.9; $p = 0.001$). In the right hemisphere, there was no significant difference in the eOA power peak latencies between the groups ($t_{(41)} = 0.3$; $p = 0.78$). The eOA power peak latencies were (in ms, mean ± SD) 85.5 ± 29.0 for patients and 57.3 ± 15.8 for normal controls in the left hemisphere, and 67.1 ± 24.1 and 69.2 ± 24.5 in the right hemisphere. For nonspeech sounds, the rmANOVA showed a significant hemisphere by group interaction ($F_{(1,41)} = 5.0$; $p = 0.03$), with no main effects ($0.3 \leq F_{(1,41)} \leq 2.9$; $0.10 \leq p \leq 0.60$). In the left hemisphere, there was no significant difference in the eOA power peak latency between groups ($t_{(41)} = 0.003$; $p = 1.0$). In the right hemisphere, patients showed significantly delayed eOA latencies ($t_{(41)} = -2.9$; $p = 0.005$). The peak latencies were 71.0 ± 16.8 for patients and 71.0 ± 20.1 for normal controls in the left hemisphere, and 80.0 ± 19.7 and 65.5 ± 12.3 in the right hemisphere, respectively. For LI of the eOA power peak latency, an rmANOVA demonstrated a significant stimulus by group ($F_{(1,41)} = 14.9$; $p < 0.001$) interaction, with no main effects ($0.8 \leq F_{(1,41)} \leq 2.6$; $0.11 \leq p \leq 0.39$). To delineate this stimulus by group interaction, the differences of LI between the groups were investigated using t tests for each stimulus. For both stimuli, patients showed the opposite hemispheric patterns to normal controls ($t_{(41)} = -3.5$, $p = 0.001$ for speech sounds; $t_{(41)} = 2.2$, $p = 0.04$ for nonspeech sounds) (Fig. 2). For the eOA phase-locking peak latency, the statistical results were the same as the results of the eOA power peak latency (Fig. 2, supplemental information and Fig. 1, available at www.jneurosci.org as supplemental material).

In summary, patients showed a delayed neural oscillatory activity to speech sounds in the left hemisphere and to nonspeech sounds in the right hemisphere, while also showing the opposite hemispheric patterns of eOA.

Mean eOA power

The mean eOA power and LI are shown in Figure 2. An rmANOVA demonstrated significant main effects of period ($F_{(2,82)} = 69.7$; $p < 0.001$) and stimulus ($F_{(1,41)} = 9.1$; $p = 0.004$), and significant hemisphere by stimulus ($F_{(1,41)} = 4.9$; $p = 0.032$), period by stimulus ($F_{(2,82)} = 22.0$; $p < 0.001$), and period by hemisphere by stimulus by group ($F_{(2,82)} = 3.6$; $p = 0.038$) interactions, with no other significant main effects or interactions ($0.09 \leq F_{(1,41)} \leq 1.2$; $0.7 \leq F_{(2,82)} \leq 2.7$; $0.08 \leq p \leq 0.77$). To delineate this period by hemisphere by stimulus by group interaction, the hemisphere factor was decomposed first.

In the left hemisphere, the rmANOVA showed a significant main effect of period ($F_{(2,82)} = 40.9$; $p < 0.001$), and significant period by group ($F_{(2,82)} = 3.7$; $p = 0.038$), period by stimulus ($F_{(2,82)} = 5.7$; $p = 0.008$), and period by stimulus by group ($F_{(2,82)} = 3.4$; $p = 0.049$) interactions, with no other significant main effects or interactions ($0.01 \leq F_{(1,41)} \leq 0.6$; $0.46 \leq p \leq 0.94$). To disentangle this period by stimulus by group interaction, follow-up rmANOVA was performed for each stimulus.

For speech sounds, the rmANOVA showed a significant main effect of period ($F_{(2,82)} = 16.4$; $p < 0.001$) and period by group ($F_{(2,82)} = 5.7$; $p = 0.009$) interaction, with no main effect of group ($F_{(1,41)} = 0.02$; $p = 0.9$). To delineate this period by group interaction, the differences of the mean eOA power between the groups were investigated using *t* tests for each period. In the 0–50 ms period, normal controls showed a significantly larger mean eOA power ($t_{(41)} = 2.2$; $p = 0.03$) than patients. In the 50–100 ms period, there was no significant difference in the mean eOA power between the groups ($t_{(41)} = 0.2$; $p = 0.88$). In the 100–150 ms period, patients showed a significantly larger mean eOA power ($t_{(41)} = -2.5$; $p = 0.02$) than normal controls. For nonspeech sounds, the rmANOVA showed a significant main effect of period ($F_{(2,82)} = 50.6$; $p < 0.001$), with no other significant main effect or interaction ($F_{(1,41)} < 0.001$; $F_{(2,82)} = 0.7$; $0.5 \leq p \leq 1.0$). The mean eOA powers in the left hemisphere to speech sounds were (in fT/cm) 22.6 ± 16.7 for patients and 36.2 ± 22.0 for normal controls in the 0–50 ms period, 43.2 ± 31.2 and 44.5 ± 23.2 in the 50–100 ms period, and 28.1 ± 21.2 and 15.1 ± 11.2 in the 100–150 ms period, and to nonspeech sounds were 23.2 ± 14.4 for patients and 27.6 ± 14.7 for normal controls,

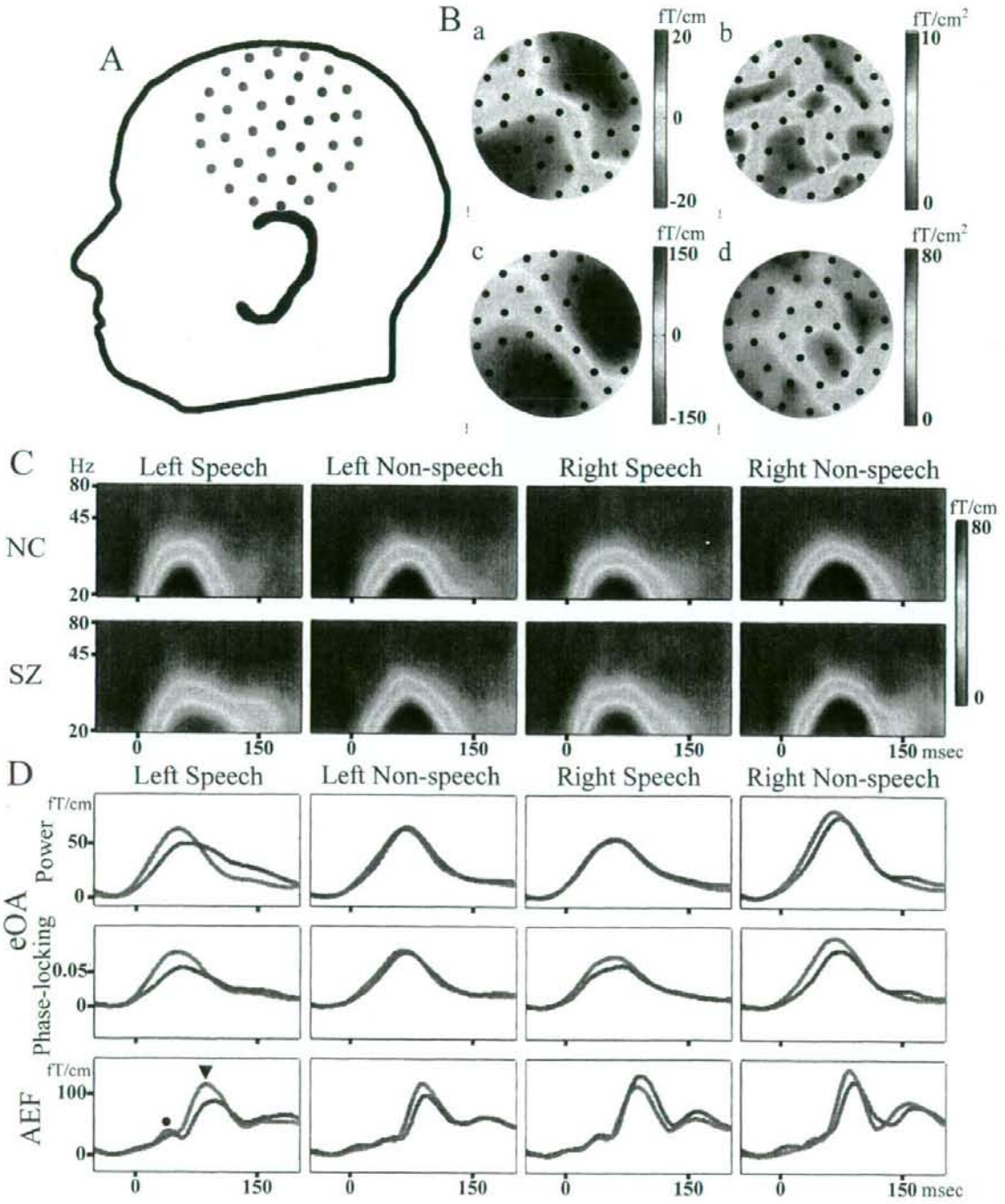

Figure 1. ***A*** and ***B*** are based on the data to speech sounds in the left hemisphere of one subject. ***A***, The layout of the measured channels. Red circles indicate the channels used for the analyses. ***Ba***, The topography of magnetic field (MF) at the eOA power peak latency. ***Bb***, Spatial derivative of ***Ba***. ***Bc***, MF of the N100m. ***Bd***, Spatial derivative of ***Bc***. Color scales signify the MF and spatial derivative. ***C***, Grand average eOA power maps to speech and nonspeech sounds in the both hemispheres. Color scale signifies eOA power. ***D***, Top, Grand average eOA power waveforms. Middle, Grand average eOA phase-locking waveforms. Bottom, Grand average auditory evoked responses. The black circle indicates the P50m, and the black triangle indicates the N100m. The waveforms of patients are shown in red and those of normal controls are shown in blue. NC, Normal controls; SZ, patients with schizophrenia; AEF, auditory evoked magnetic field.

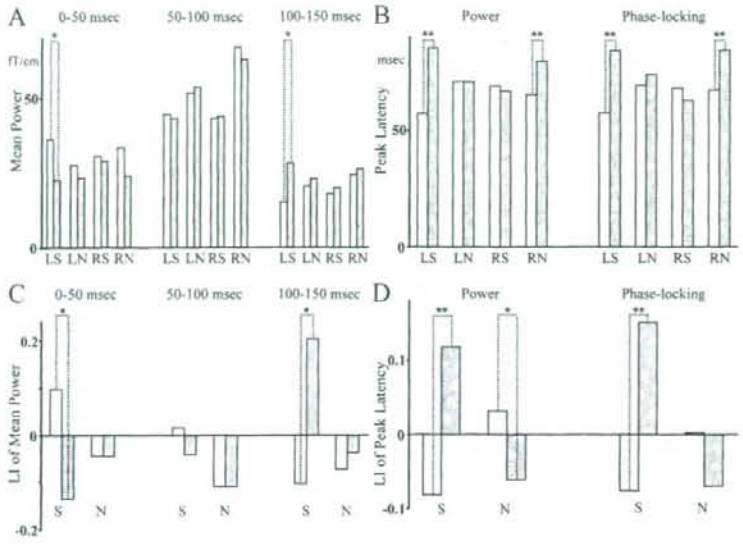

Figure 2. *A*, The mean eOA power. *B*, The eOA power and phase-locking peak latency. *C*, LI of *A*. *D*, LI of *B*. L and R are the left and right hemisphere, and S and N are speech and nonspeech sounds, respectively. The data of patients are shown as dotted bars and those of normal controls are shown as plain bars. $^{**}p < 0.01$; $^{*}p < 0.05$.

53.7 ± 29.2 and 51.7 ± 25.6, and 22.9 ± 13.1 and 20.4 ± 11.2, respectively.

In the right hemisphere, the rmANOVA demonstrated a significant main effects of period ($F_{(2,82)} = 55.2$; $p < 0.001$) and stimulus ($F_{(1,41)} = 11.3$; $p = 0.002$), and a significant period by stimulus ($F_{(2,82)} = 20.1$; $p < 0.001$) interaction, with no other significant main effects or interactions ($0.2 \leq F_{(1,41)} \leq 0.6$; $0.6 \leq F_{(2,82)} \leq 0.7$; $0.43 \leq p \leq 0.67$). The mean eOA powers in the right hemisphere to speech sounds were (in fT/cm) 29.0 ± 17.9 for patients and 30.6 ± 24.5 for normal controls in the 0–50 ms, 43.9 ± 22.3 and 43.2 ± 22.7 in the 50–100 ms, and 19.9 ± 15.6 and 18.0 ± 10.2 in the 100–150 ms, and to nonspeech sounds were 23.9 ± 12.9 for patients and 33.4 ± 23.6 for normal controls, 62.9 ± 27.8 and 67.0 ± 33.8, and 26.2 ± 16.3 and 24.4 ± 13.0, respectively.

For the LI of the mean eOA power, an rmANOVA demonstrated a significant period by group ($F_{(2,82)} = 3.6$; $p = 0.04$) and period by stimulus by group ($F_{(2,82)} = 5.4$; $p = 0.01$) interactions, with no other significant main effects or interactions ($0.005 \leq F_{(1,41)} \leq 2.2$; $0.58 \leq F_{(2,82)} \leq 0.61$; $0.15 \leq p \leq 0.95$). To delineate this period by stimulus by group interaction, a follow-up rmANOVA was performed for each stimulus. For speech sounds, an rmANOVA demonstrated a significant period by group ($F_{(2,82)} = 7.9$; $p = 0.003$) interaction, with no main effects ($F_{(1,41)} = 0.003$; $F_{(2,82)} = 0.6$; $0.49 \leq p \leq 0.96$). To delineate this period by group this interaction, the differences in the LI between the groups were investigated using *t* tests for each period. Patients showed the opposite hemispheric patterns to normal controls in the 0–50 ms and 100–150 ms periods, with no difference in the 50–100 ms period (0–50 ms period, $t_{(41)} = 2.1$, $p = 0.04$; 50–100 ms period, $t_{(41)} = 0.5$, $p = 0.62$; 100–150 ms period, $t_{(41)} = -2.2$, $p = 0.03$) (Fig. 2). We also used the other baseline (from −100 to −50 ms) for the analyses to confirm the results, and the statistical results were the same using both baselines.

In summary, patients showed a significantly smaller neural oscillatory activity in the 0–50 ms period and a significantly larger activity in the 100–150 ms in the left hemisphere to speech sounds specifically, and showed opposite hemispheric patterns of eOA to speech sounds in the two periods. The results of eOA in 45–80 Hz are presented in the supplemental material (available at www.jneurosci.org).

P50m and N100m

For the P50m amplitude, an rmANOVA demonstrated a significant main effect of stimulus ($F_{(1,41)} = 8.9$; $p = 0.005$), with no other significant main effects or interactions ($0.07 \leq F_{(1,41)} \leq 2.4$; $0.13 \leq p \leq 0.79$). For the P50m latency, there were no significant main effects or interactions ($0.001 \leq F_{(1,41)} \leq 0.9$; $0.35 \leq p \leq 0.97$).

For the N100m amplitude, an rmANOVA demonstrated a significant main effect of hemisphere ($F_{(1,41)} = 5.3$; $p = 0.03$), with no other significant main effects or interactions ($0.2 \leq F_{(1,41)} \leq 3.6$; $0.07 \leq p \leq 0.69$). For the N100m latency, there were a significant main effect of stimulus ($F_{(1,41)} = 11.1$; $p = 0.002$), but no other significant main effects or interactions ($0.004 \leq F_{(1,41)} \leq 3.2$; $0.08 \leq p \leq 0.95$). These results indicated that there were no significant group differences in the P50m and the N100m of the conventional evoked responses.

Correlations between eOA power and auditory hallucination

A significant negative correlation was observed between the mean eOA power to speech sounds in the 100–150 ms period in the left hemisphere and the auditory hallucination scores in SAPS (rho = −0.51; $p = 0.023$), but no significant correlations between the eOA power peak latency to speech sounds in the left hemisphere, those to nonspeech sounds in the right hemisphere, nor any LI of these indices ($-0.41 \leq$ rho ≤ 0.19; $0.07 \leq p \leq 1.0$) (Fig. 3).

Discussion

The major findings of this study were as follows: (1) patients showed a delayed neural oscillatory activity to speech sounds in the left hemisphere and to nonspeech sounds in the right hemisphere; (2) in the 0–50 ms period, patients showed significantly reduced eOA power to speech sounds in the left hemisphere; (3) in the 100–150 ms period, patients showed significantly larger eOA power to speech sounds in the left hemisphere; (4) patients showed the opposite hemispheric patterns in eOA peak latency to both sounds and the opposite hemispheric patterns in eOA to speech sounds; (5) the eOA power in 100–150 ms period to speech sounds in the left hemisphere was associated with auditory hallucinations.

Abnormal eOA to speech sounds in schizophrenia

Näätänen et al. (1997) reported the existence of a cortical language-specific automatic detection system indexed by the mismatch negativity. This system is formed within the first year of life (Cheour et al., 1998) and it has been hypothesized to underlie the activation of the speech-specialized network in the left hemisphere. Based on these studies, Palva et al. (2002) stated that the different MEG patterns of the eOA at 20–45 Hz to speech and nonspeech sounds in humans might reflect the activation of the

left-hemispheric language-specialized network. The results of the current study suggest that patients with schizophrenia may have deficits in a fast mechanism for identifying speech sounds, related to an impaired left hemispheric language-specific neural system. Moreover, in the present study, the analyses of the lateralization index revealed the pattern of hemispheric lateralization to be the opposite in patients. A reversal in normal lateralization may therefore be closely related to the pathology of schizophrenia.

For the eOA-symptom correlation, the increased severity of auditory hallucinations was associated with smaller eOA to speech sounds in the left hemisphere in the 100–150 ms period. The results of the current study indicate that this abnormal neural oscillatory activity to speech sounds may underlie the generation of auditory hallucinations in schizophrenia; however, this finding warrants confirmation in a larger sample.

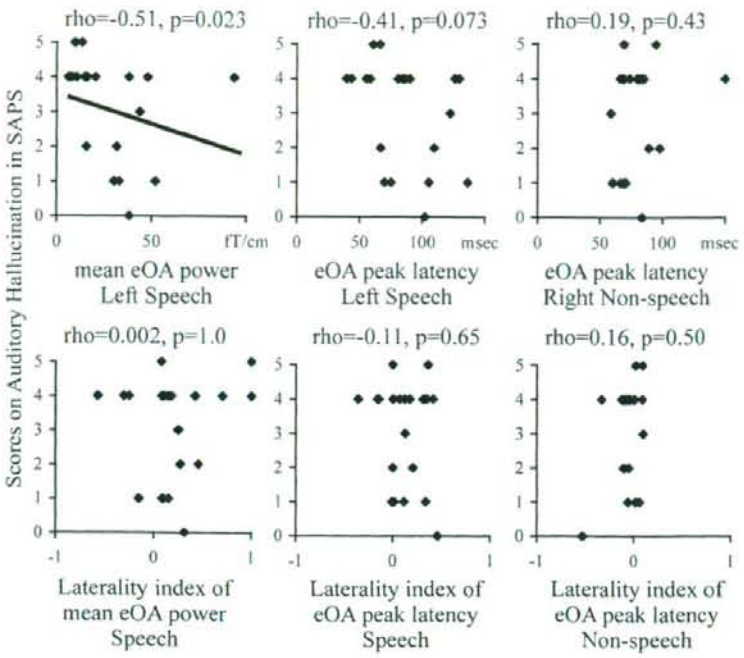

Figure 3. Scattergrams between the mean eOA powers to speech sounds in the left hemisphere in the 100–150 ms period, the eOA power peak latency to speech sounds in the left hemisphere, the eOA power peak latency to nonspeech sounds in the right hemisphere and the LI of these indices, and the scores of auditory hallucinations.

Generation of the eOA at 20–45 Hz

Previous *in vitro* studies have suggested that beta2 oscillations (20–30 Hz) are different from gamma oscillations (30–45 Hz) in terms of generation. For gamma oscillations, Cunningham et al. (2004) reported that the fast rhythmic bursting neurons in layer II/III play a crucial role in the generation of gamma oscillations. GABAergic neurons have been reported to play a crucial role in the primary generation of gamma oscillations and their local synchronization (Traub et al., 2004). In addition, direct electronic coupling through gap junctions between inhibitory neurons also contributes to the synchronization of the gamma oscillations (Traub et al., 2001). For beta oscillations, *in vitro* study by Roopun et al. (2006) reported that beta2 oscillations occurred in layer V pyramidal cells. Moreover, this study indicated that beta2 oscillations are involved in gap junctional coupling and independent of chemical synaptic transmission. The present study suggests that schizophrenia may be characterized by a left hemisphere-selective impaired neural circuitry for speech detection, and this functional deficit, at the cellular level, may be associated with a reduction of GABA interneurons and/or an abnormality in gap junctions.

Previous studies on eOA in schizophrenia

To our knowledge, this is the first study to demonstrate abnormal eOA to speech sounds in schizophrenia. Kwon et al. (1999) reported reduced 40 Hz steady-state eOA and showed delayed phase synchronization/desynchronization to the click train in schizophrenia. MEG offers high spatial resolution to detect neuronal activity to auditory stimuli (Onitsuka et al., 2000) and, thus, MEG is suited to evaluate the hemispheric differences in eOA. Because the 40 Hz entrained EEG response to auditory stimuli is largest at the middle frontal electrode sites and unfit to detect hemispheric differences, it is the novel finding of the current study that patients showed a delayed neural oscillatory activity to speech sounds in the left hemisphere and to nonspeech sounds in the right hemisphere. It will be important to clarify the association between the delayed eOA latency of the present study and the delayed phase synchronization/desynchronization to the click train in the same samples.

As noted above, there is a difference in the generation between beta2 and gamma oscillations. Therefore, the findings in eOA studies for schizophrenia should be carefully interpreted, because some of these studies have investigated high-frequency oscillations including both beta and gamma band oscillations (Blumenfeld and Clementz, 2001).

Conclusion

These results indicated that patients showed different characteristics of eOA compared with normal controls, probably related to deficits in a fast mechanism for identifying speech sounds, and the abnormal neural circuit function in speech recognition may be an underlying pathophysiology of schizophrenia. Moreover, the present study suggested that schizophrenia might be characterized by an opposite pattern of hemispheric lateralization in auditory evoked oscillations.

References

Bastiaansen MC, Knösche TR (2000) Tangential derivative mapping of axial MEG applied to event-related desynchronization research. Clin Neurophysiol 111:1300–1305.

Belin P, Zatorre RJ, Lafaille P, Ahad P, Pike B (2000) Voice-selective areas in human auditory cortex. Nature 403:309–312.

Blumenfeld LD, Clementz BA (2001) Response to the first stimulus determines reduced auditory evoked response suppression in schizophrenia: single trials analysis using MEG. Clin Neurophysiol 112:1650–1659.

Cheour M, Ceponiene R, Lehtokoski A, Luuk A, Allik J, Alho K, Näätänen R (1998) Development of language-specific phoneme representations in the infant brain. Nat Neurosci 5:351–353.

Cunningham MO, Whittington MA, Bibbig A, Roopun A, LeBeau FE, Vogt A, Monyer H, Buhl EH, Traub RD (2004) A role for fast rhythmic burst-

ing neurons in cortical gamma oscillations *in vitro*. Proc Natl Acad USA 101:7152–7157.

Gallinat J, Winterer G, Herrmann CS, Senkowski D (2004) Reduced oscillatory gamma-band responses in unmedicated schizophrenic patients indicate impaired frontal network processing. Clin Neurophysiol 115:1863–1874.

Haig AR, Gordon E, Pascalis VD, Meares RA, Bahramali H, Harris A (2000) Gamma activity in schizophrenia: evidence of impaired network binding? Clin Neurophysiol 111:1461–1468.

Herrmann CS, Munk MH, Engel AK (2004) Cognitive functions of gamma-band activity: memory match and utilization. Trends Cogn Sci 8:347–355.

Hong LE, Summerfelt A, McMahon R, Adami H, Francis G, Elliott A, Buchanan RW, Thaker GK (2004) Evoked gamma band synchronization and the liability for schizophrenia. Schizophr Res 70:293–302.

Kiebel SJ, Tallon-Baudry C, Friston KJ (2005) Parametric analysis of oscillatory activity as measured with EEG/MEG. Hum Brain Mapp 26:170–177.

Kircher TT, Rapp A, Grodd W, Buchkremer G, Weiskopf N, Lutzenberger W, Ackermann H, Mathiak K (2004) Mismatch negativity responses in schizophrenia: a combined fMRI and whole-head MEG study. Am J Psychiatry 161:294–304.

Kwon JS, O'Donnel BF, Wallenstein GV, Greene RW, Hirayasu Y, Nestor PG, Hasselmo ME, Potts GF, Shenton ME, McCarley RW (1999) Gamma frequency-range abnormalities to auditory stimulation in schizophrenia. Arch Gen Psychiatry 56:1001–1005.

Näätänen R, Lehtokoski A, Lennes M, Cheour M, Huotilainen M, Iivonen A, Vainio M, Alku P, Ilmoniemi RJ, Luuk A, Allik J, Sinkkonen J, Alho K (1997) Language-specific phoneme representations revealed by electric and magnetic brain responses. Nature 385:432–434.

Nestor PG, Han SD, Niznikiewicz M, Salisbury DF, Spencer KM, Shenton ME, McCarley RW (2001) Semantic disturbance in schizophrenia and its relationship to the cognitive neuroscience of attention. Biol Psychol 57:23–46.

Onitsuka T, Ninomiya H, Sato E, Yamamoto T, Tashiro N (2000) The effect of interstimulus intervals and between-block rests on the auditory evoked potential and magnetic field: is the auditory P50 in humans an overlapping potential? Clin Neurophysiol 111:237–245.

Palva S, Palva JM, Shtyrov Y, Kujala T, Ilmoniemi RJ, Kaila K, Näätänen R (2002) Distinct gamma-band evoked responses to speech and non-speech sounds in humans. J Neurosci 22:RC211(1–5).

Roopun AK, Middleton SJ, Cunningham MO, LeBeau FE, Bibbig A, Whittington MA, Traub RD (2006) A beta2-frequency (20–30 Hz) oscillation in non synaptic networks of somatosensory cortex. Proc Natl Acad USA 103:15646–15650.

Spencer KM, Nestor PG, Niznikiewicz MA, Salisbury DF, Shenton ME, McCarley RW (2003) Abnormal neural synchrony in schizophrenia. J Neurosci 23:7407–7411.

Spencer KM, Nestor PG., Perlmutter R, Niznikiewicz MA, Klump MC, Frumin M, Shenton ME, McCarley RW (2004) Neural synchrony indexes disordered perception and cognition in schizophrenia. Proc Natl Acad USA 101:17288–17293.

Tallon-Baudry C, Bertrand O, Delpuech C, Pernier J (1996) Stimulus specificity of phase-locked and non-phase-locked 40 Hz visual responses in human. J Neurosci 16:4240–4249.

Traub RD, Koppell N, Bibbig A, Buhl EH, LeBeau FE, Whittington MA (2001) Gap junctions between interneuron dendrites can enhance synchrony of gamma oscillations in distributed networks. J Neurosci 21:9478–9486.

Traub RD, Bibbig A, LeBeau FE, Buhl EH, Whittington MA (2004) Cellular mechanisms of neuronal population oscillation in the hippocampus *in vitro*. Annu Rev Neurosci 27:247–278.

Uhlhaas PJ, Singer W (2006) Neural synchrony in brain disorders: relevance for cognitive dysfunctions and pathophysiology. Neuron 52:155–168.

Uhlhaas PJ, Linden DE, Singer W, Haenschel C, Lindner M, Maurer K, Rodriguez E (2006) Dysfunctional long-range coordination of neural activity during Gestalt perception in schizophrenia. J Neurosci 26:8168–8175.

Available online at www.sciencedirect.com
ScienceDirect
Psychiatry Research: Neuroimaging 163 (2008) 260–269
PSYCHIATRY RESEARCH NEUROIMAGING
www.elsevier.com/locate/psychresns

Auditory sensory gating to the human voice: A preliminary MEG study

Yoji Hirano[a], Toshiaki Onitsuka[a,*], Toshihide Kuroki[a], Yuji Matsuki[b], Shogo Hirano[a], Toshihiko Maekawa[a], Shigenobu Kanba[a]

[a]*Department of Neuropsychiatry, Graduate School of Medical Sciences, Kyushu University, Fukuoka, Japan*
[b]*Department of Intelligent Systems, Faculty of Information Science and Electrical Engineering, Kyushu University, Fukuoka, Japan*

Received 4 July 2006; received in revised form 25 June 2007; accepted 16 July 2007

Abstract

The ability of the brain to suppress incoming irrelevant sensory input is termed 'sensory gating,' and auditory sensory gating is often indexed by the auditory evoked response. We recorded the auditory evoked magnetic fields to the human voice, using the conditioning–testing paradigm, to investigate whether or not healthy subjects show less activation to the second voice stimulus. Seventeen healthy adults (mean age 27.9±4.8 years, 9 males and 8 females) participated in the experiment. The auditory stimuli were presented monaurally as a series of 120 paired voices, with 500-ms interstimulus intervals and 6-s interpaired stimulus intervals. The P50m and the N100m responses were investigated, and dipole source localization was performed. Root mean squares of both P50m and N100m were significantly suppressed to the second stimulus bilaterally, and the suppression was more significant in N100m. The N100m was located significantly more laterally than the P50m for both hemispheres. These results therefore demonstrate the presence of sensory gating for auditory inputs of the human voice in the primary auditory cortex and the auditory association area.

Keywords: P50m; Human voice; Sensory gating; Magnetoencephalography

1. Introduction

Sensory gating is often indexed by evoked potentials such as P50, which is a positive potential at around 50 ms elicited by auditory stimuli. The P50 component has recently become the focus of clinical interest in patients with various mental diseases (Adler et al., 1982; Freedman et al., 1983; Buchwald et al., 1989, 1992; Neylan et al., 1999; Jessen et al., 2001). Using a conditioning–testing paradigm, Adler et al. (1982) reported that patients with schizophrenia showed deficits in sensory gating indexed by decreased P50 inhibition to the second auditory stimulus. However, the published reports of P50 generation are mixed, and generators of P50 in the human brain still remain unclear. For example, Lee et al. (1984) have recorded P50 from subdural electrodes and have reported that human P50 is a near-field potential in the primary auditory cortex. On the other hand, P50 is sensitive to the level of arousal (Erwin and Buchwald, 1986), thus suggesting that P50 is from the ascending reticular activating system. It has been reported that human scalp P50 may be an overlapping

* Corresponding author. Department of Neuropsychiatry, Graduate School of Medical Sciences, Kyushu University, 3-1-1, Maidashi, Higashiku, Fukuoka, 812-8582, Japan. Tel.: +81 92 642 5627; fax: +81 92 642 5644.
E-mail address: toshiaki@npsych.med.kyushu-u.ac.jp (T. Onitsuka).

0925-4927/$ - see front matter © 2007 Elsevier Ireland Ltd. All rights reserved.
doi:10.1016/j.pscychresns.2007.07.002

ial (Cacace et al., 1990; Ninomiya et al., 1997; ıka et al., 2000). Huang et al. (2003) reported that ıle generators contributed to the scalp P50 in ts with schizophrenia.

other regions involved in sensory gating, the campus has been reported to play a crucial role in ditory sensory gating system (Krause et al., 2003; vald et al., 2003; Boutros et al., 2005). Of note, vald et al. (2003) reported that habituating auditory d responses in the neocortex and the hippocampus d around 50 ms and 250 ms, respectively. They ıde that such sensory gating may therefore be a tep process subserved by different brain areas.

gnetoencephalography (MEG) offers high spatial tion to accurately locate the position of neuronal y to auditory stimuli compared with electroen- lography (EEG) (Yamamoto et al., 1988). EEG cord activity in the subcortex as well as in the ry cortex (Cacace et al., 1990; Onitsuka et al., whereas MEG can predominantly detect auditory ıl response, since MEG is sensitive to the current ıents flowing tangentially with respect to the surface (Huizenga et al., 2001). In the MEG ıre, P50m (the magnetic counterpart of P50) has eported to be generated in or near the primary ry cortex (Mäkelä et al., 1994; Yoshiura et al., Kanno et al., 2000; Onitsuka et al., 2000; Godey 2001). In addition, Godey et al. (2001) reported e P50m source was localized in the lateral part of l's gyrus (HG). It may therefore be important to igate auditory sensory gating in the human ry cortex using MEG with a conditioning–testing gm, since the source of auditory evoked responses en clear in MEG.

ditory stimuli also elicit a negative potential l N100, which is one of the best-investigated ry evoked responses with a negative peak at imately 100 ms after auditory stimuli. N100 se arises from the primary and auditory associ- ıreas (Jacobson et al., 1997). In MEG studies, it en reported that N100m is located in the auditory ation area (planum temporale [PT]) (Pantev et al., Lütkenhöner and Steinsträter, 1998).

ently, functional magnetic resonance imaging) studies have revealed that human voices are ved, at least in part, by a processing stream te from that used in processing other non-vocal nmental sounds (Belin et al., 2000). More ically, the bilateral superior temporal sulcus regions have been reported to selectively respond human voice (Belin et al., 2000; Fecteau et al., As noted before, patients with schizophrenia may have deficits for auditory sensory gating. Schizophrenic patients often show auditory hallucinations of the human voice, which may be related to a reduced gray matter volume of left superior temporal gyrus (STG) including the HG and the PT (Onitsuka et al., 2004). It will therefore be important to investigate sensory gating in the human voice. The present study was designed to investigate whether or not healthy subjects show less activation to the second voice stimulus with a conditioning–testing paradigm, which supports sensory gating to the human voice in the auditory cortex.

2. Methods

2.1. Subjects

Seventeen healthy adults (mean age 27.9±4.8 years, range 21 to 38; 9 males and 8 females) participated in the experiment. Handedness was assessed using the Edinburgh inventory, and all subjects were right-handed (the score of handedness: 94.6±11.6) (Oldfield, 1971). The subjects were screened using the Structured Clinical Interview (SCID) — non-patient edition (Spitzer et al., 1990). To rule out otolaryngologic disorders, the subjects were also screened with a questionnaire assessing physical condition and past history, and a brief physical examination for hearing was performed. None of the subjects had either an Axis-I psychiatric disorder or otolaryngologic disorders. After a complete description of the study, all participants signed an informed consent form in accordance with the regulations of the Ethic commission of the Graduate School of Medical Sciences, Kyushu University.

2.2. Stimulation and procedures

During the experiment, all subjects were in the lateral recumbent position on a bed in a magnetically shielded room (Sumitomo Metal Ind., Ltd.) at Kyushu university Hospital. Auditory evoked responses in both hemispheres were recorded alternately. The subjects were instructed to keep their eyes open and not to sleep. The Japanese vowel sound /a/ was used as an auditory voice stimulus. The stimulus was the voice spoken by an actor who was a native Japanese speaker, and was digitized and edited with 200-ms duration (rise/fall 10 ms). The frequencies for the formants (F) of the vowel /a/ were as follows: FO=140 Hz, F1=760, F2=1250, F3=2750, F4=3600. At the earpiece, the intensity of the stimulus was 60 dB sound pressure level.

The software for stimulus generation was run on a mini-computer (NEC PC-9801FA). The software

controlled interstimulus intervals (between conditioning–testing stimuli) (ISI) and inter paired-stimulus interval (IPI), and provided a trigger signal at every stimulus onset. Stimuli were delivered to the ear contralateral to the hemisphere being recorded through a 2.3-m plastic tube with a plastic insert earpiece at the tip. The stimuli were presented consecutively as a series of 120 paired voice stimuli with 500-ms ISI and 6-s IPI. The order of the recorded hemisphere was counterbalanced between the subjects.

2.3. Data acquisition and analysis

A 37-channel biomagnetometer (Magnes, Biomagnetic Technologies Inc., San Diego, CA) was used for the magnetic measurements. The sensing coils consisted of first-order axial gradiometers, measuring 20 mm in diameter, with a baseline of 50 mm, and the distance of the center between adjacent coils was 22 mm. The coils were arranged uniformly in concentric circles over a spherical surface covering a circle of 14.4 cm in diameter with a 12-cm radius. To define the head shape of each subject in 3-dimension (3D) for dipole source localization, the head shape was traced using 3D digitizer. The sensor was positioned over the left and the right temporal region of the subject, and remained in the same position for each hemisphere. The location of these coils in relation to the preauricular points and nasion were determined with a 3D digitizer before the start of data acquisition.

All signals were digitized at 4167 Hz and stored in a magneto-optical disk. The data were collected and analyzed using a software package (MSI software, WHS version 1.2.4, Biomagnetometer system) on a workstation (SUN, SPARC Station™). In the off line analysis, the MEG was triggered by stimulus onset with a sampling rate of 4167 Hz and it was averaged for each condition. Epochs with signal variations exceeding 4.0 pT were excluded from averaging. The epochs were of 400-ms duration including a 100-ms prestimulus interval. The final responses were filtered with between 1 and 100 Hz using a sharp digital bandpass filter with a slope of 12 dB/oct and the digital 60-Hz notch filter which selectively cut the 60-Hz band. A pre-stimulus baseline correction was performed using the averaged activity during the 100-ms prestimulus interval for each channel. For each component, an assessment of the global magnetic field at the peak latency was carried out using the root mean square (RMS) values across the 37 channels of MEG data with the following formula; $RMS(t)=[\Sigma x(i,t)^2/37]^{0.5}$, where $x(i,t)$ is the value of magnetic field for each channel ($i=1$ to 37) at time t and $\Sigma x(i,t)^2/37$ is the square mean of the magnetic field of 37 channels. The N100m peak latency was defined as the latency with the largest amplitude between 80 and 120 ms following stimulus onset. We always referred to isomagnetic contour maps of P50m and N100m to observe the polarity information (see Supplement 1). The P50m peak latency was also defined between 20 and 70 ms, where the P50m showed the reversed polarity to the N100m. When we observed multiple peaks, the largest amplitude was referred to as the peak of the response.

In the present study, the dipole sources of the P50m and the N100m to the first stimulus (S1) were calculated. In addition, we also performed source localization analyses on the difference subtracted the second response (S2) from the first response (S1–S2). We used a single equivalent current dipole analysis based on the non-linear inverse problem with the least squares search (Sarvas, 1987), and the best fit single equivalent dipole was estimated every 0.5 ms using a software program (MSI software, WHS version 1.2.4, Biomagnetometer system) on a workstation (SUN, SPARC Station™). We calculated the correlation coefficient between the theoretical field generated by the estimated equivalent dipole model and the observed field for P50m and N100m. The correlation coefficients indicate how closely the measured values correspond to the theoretical field generated by the model. When the calculated correlation coefficient was less than 0.90, we determined that the single equivalent dipole was not observed. The dipole locations, moments and directions of P50m and N100m were calculated at the latency where the correlation coefficient was a maximum level. A spherical model was fitted to the digitized head shape of each subject and then the dipole locations were expressed by x, y and z-coordinates. The zero point was the exact mid-point of the line between the bilateral preauricular points. The x-axis was the antero-posterior line with a positive x-axis extended from the zero point toward the nasion. The y-axis was the line from the right preauricular point to the left with positive y-axis extended from the zero point toward the left preauricular point. The (vertical) z-axis was the line orthogonal to both the x-axis and y-axis with positive z-axis extended from the zero point toward the upper side.

T1-weighted coronal MR images of eight subjects were acquired with contiguous (no-gap) 5-mm slice thickness using a Toshiba (MRT-50A) 0.5 T system. In order to overlay the calculated dipoles onto the MRI of the subject's brain, the nasion and bilateral preauricular points were identified on the MRI images by registering the fiduciary points and the traced points over the scalp to MRI imaging.

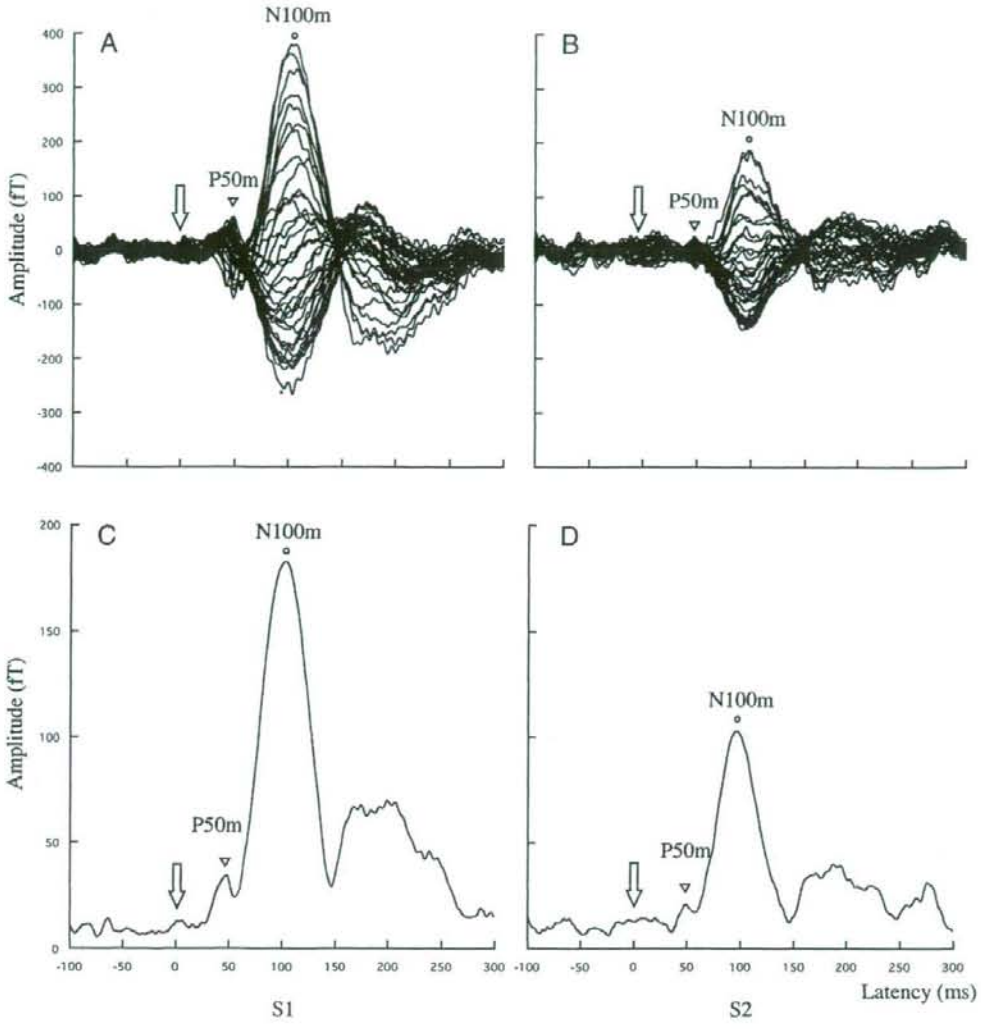

The auditory evoked magnetic responses to S1 and S2 from one subject. The MEG waveforms to S1 (A) and S2 (B), obtained by the position of all 37 channels. The RMS waveforms to S1 and S2 are shown in (C) and (D), respectively. The triangles indicate P50m, and the indicate N100m. The arrows signify the onset of the stimulus.

atistical analysis

peak RMS or the peak latency values of the and N100m were submitted to repeated measures 'A with stimulus type (S1 or S2), hemisphere (left t) and component (P50m or N100m) as within- s factors. To assess the difference in the source n between P50m and N100m, we investigated the ns of the statistically significant P50m and n dipoles to S1. A repeated measures MANOVA xis (x, y or z) and component (P50m or N100m) hin-subjects factors was performed for each here. Finally, to assess any differences in the source location between the S1 and the S1–S2 responses, we investigated the locations of the statistically significant P50m and N100m dipoles. A repeated measures MANOVA with axis (x, y or z) and response (S1 or S1–S2) as within-subjects factors was performed for each hemisphere and each component.

3. Results

The numbers of epochs for averaging were 117±7 (mean±S.D.) for S1 and 116±7 for S2 in the left hemisphere, and 116±10 for S1 and 116±11 for S2 in the right hemisphere, with no significant difference

Table 1
Latency and RMS of P50m and N100m to the first (S1) and second (S2) stimuli for each hemisphere

			S1	S2	*df*	*t*	*P*
P50m	Left	Latency (ms)	48.5±11.2	47.1±7.3	16	0.48	0.64
		RMS (fT)	38.1±13.4	29.5±9.5	16	3.08	0.07
	Right	Latency (ms)	44.7±8.3	45.8±7.3	16	−0.55	0.59
		RMS (fT)	34.8±15.2	28.8±12.9	16	1.49	0.16
N100m	Left	Latency (ms)	97.7±9.9	86.7±17.7	16	2.48	0.03
		RMS (fT)	132.8±37.1	81.5±34.8	16	7.71	<0.001
	Right	Latency (ms)	93.0±8.1	88.2±10.9	16	1.53	0.15
		RMS (fT)	144.5±47.3	81.0±40.2	16	7.31	<0.001

(one-way ANOVA, $F[3,64]=0.08$, $P=0.97$). All of the subjects had P50m and N100m peaks to S1 and S2. For the left hemisphere, the number of peaks between 20 and 70 ms was as follows: a single peak (11 out of 17 subjects for S1 and 4 for S2), two peaks (5, 10), three peaks (1, 3). For the right hemisphere, the number of peaks was as follows: a single peak (11 for S1 and 9 for S2), two peaks (6, 7), three peaks (0, 1). The largest RMS amplitude with the reversed polarity to the N100m at the range was defined as the P50m RMS. Fig. 1 shows the auditory evoked magnetic responses to S1 and S2 from one subject.

3.1. RMS of P50m and N100m

The latency and RMS of P50m and N100m are shown in Table 1. Fig. 2 shows scattergrams of RMS to S1 and S2. A repeated measures ANOVA demonstrated significant main effects of stimulus ($F[1,16]=86.2$, $P<0.001$) and component ($F[1,16]=124.6$, $P<0.001$), but no main effect of hemisphere ($F[1,16]=0.2$, $P=0.69$). No significant stimulus-by-hemisphere-by-component ($F[1,16]=2.2$, $P=0.16$), stimulus-by-hemisphere ($F[1,16]=0.8$, $P=0.38$), hemisphere-by-component ($F[1,16]=0.9$, $P=0.36$) interactions were observed. However, there was a significant stimulus-by-component interaction ($F[1,16]=59.3$, $P<0.001$). To further delineate the source of the stimulus-by-component interaction, we performed post hoc repeated measures ANOVAs with stimulus and hemisphere as within-subject factors for each component.

For P50m, repeated measures ANOVA demonstrated a significant main effect of the stimulus ($F[1,16]=7.7$, $P=0.01$), but no main effect of the hemisphere ($F[1,16]=0.8$, $P=0.40$) and no significant stimulus-by-hemisphere interaction ($F[1,16]=0.3$, $P=0.57$), thus indicating that P50m to the second stimulus was significantly suppressed in both hemispheres. For N100m, a repeated measures ANOVA demonstrated a significant main effect of stimulus ($F[1,16]=85.6$, $P<0.001$), but no main effect of hemisphere ($F[1,16]=0.5$, $P=0.50$) and no significant stimulus-by-hemisphere interaction ($F[1,16]=1.7$, $P=0.21$), thus indicating that the second stimulus was suppressed significantly in both hemispheres. In summary, both P50m and N100m showed significant suppression to the second stimulus, and the suppression was more significant in N100m.

3.2. Latency of P50m and N100m

Repeated measures ANOVA demonstrated a trend-level main effect of stimulus ($F[1,16]=4.1$, $P=0.06$) and no main effect of hemisphere ($F[1,16]=1.2$, $P=0.29$). No significant stimulus-by-hemisphere-by-component ($F[1,16]=0.4$, $P=0.51$), stimulus-by-hemisphere ($F[1,16]=1.6$, $P=0.23$), hemisphere-by-component ($F[1,16]=0.1$, $P=0.79$) interactions. However, there was a significant stimulus-by-component interaction ($F[1,16]=9.7$, $P=0.007$). To further delineate the source of the stimulus-by-component interaction, we performed post hoc repeated measures ANOVAs with stimulus and hemisphere as within-subjects factors for each component.

For P50m, there were no main effects of stimulus ($F[1,16]=0.004$, $P=0.95$), hemisphere ($F[1,16]=1.0$, $P=0.33$), and no stimulus-by-hemisphere interaction ($F[1,16]=0.6$, $P=0.46$), thus indicating no stimulus effect to P50m latency. For N100m, a repeated measures ANOVA demonstrated a significant main effect of stimulus ($F[1,16]=8.4$, $P=0.01$), but no main effect of hemisphere ($F[1,16]=0.5$, $P=0.51$) and no significant stimulus-by-hemisphere interaction ($F[1,16]=1.3$, $P=0.26$), thus indicating that the N100m latency of the second stimulus was earlier than the first one.

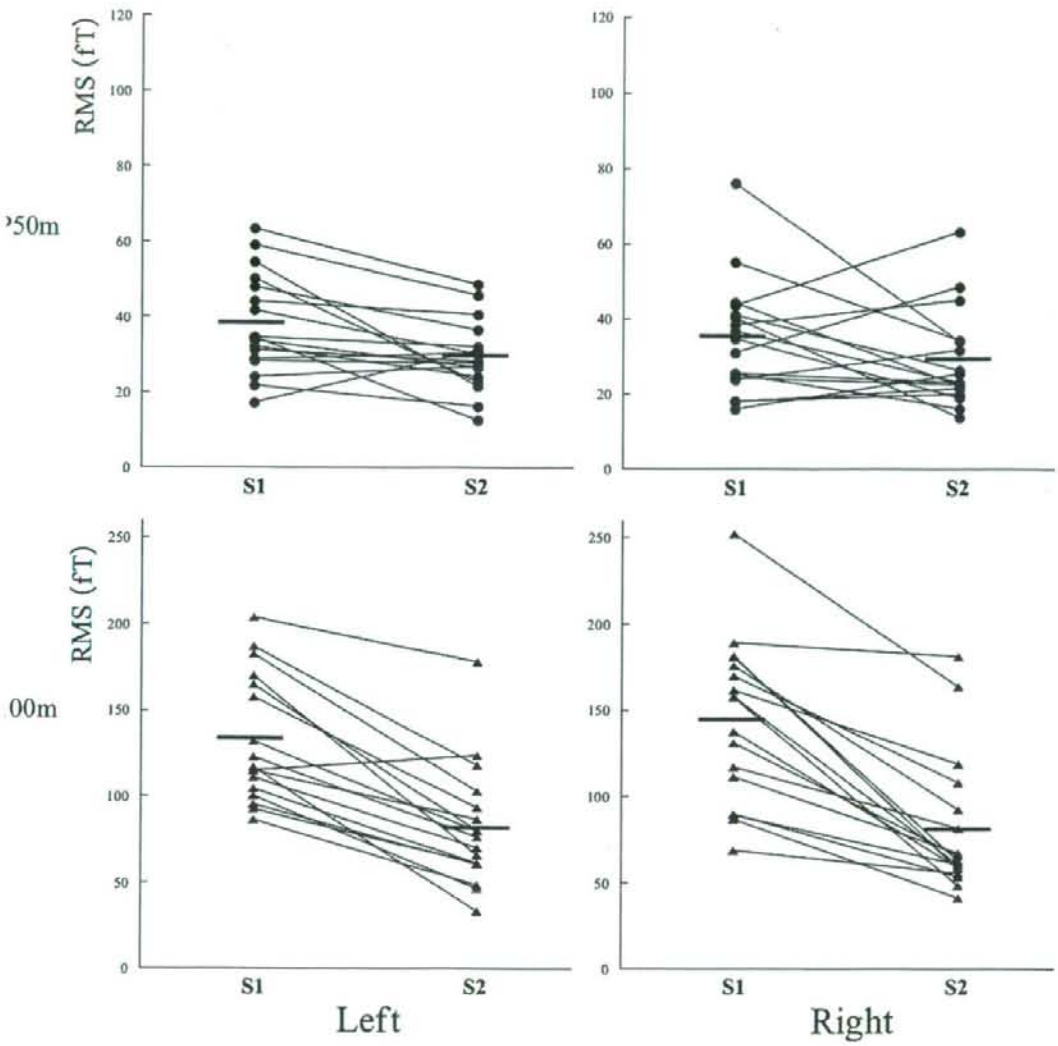

Scattergrams of RMS of P50m and N100m to the first (S1) and the second (S2) stimuli in both hemispheres. The means are indicated by tal lines.

he dipole sources of P50m and N100m

rteen subjects had statistically significant P50m 100m dipoles to the first stimulus. The *x*, *y*, and dinates of P50m and N100m are shown in Table r the left hemisphere, a repeated measures OVA demonstrated a significant component-by- iteraction ($F[2,11]=10.1$, $P=0.003$) but no main of the component ($F[1,12]=2.6$, $P=0.13$). To delineate this interaction, we performed paired for each axis. There was a significant difference *y*-coordinate ($t[12]=-3.9$, $P=0.002$), thus ting that N100m was located significantly laterally than P50m. There was no difference in the *x*-coordinate ($t[12]=1.1$, $P=0.31$) or the *z*-coordinate ($t[12]=0.4$, $P=0.67$). For the right hemisphere, a repeated measures MANOVA demonstrated

Table 2
The dipole location of P50m and N100m to the first stimulus for each hemisphere ($n=13$)

		P50m	N100m	*df*	*t*	*P*
Left	*x* (cm)	0.13±0.93	−0.62±0.77	12	1.05	0.31
	y (cm)	4.26±1.25	5.66±0.47	12	−3.86	0.01
	z (cm)	5.27±1.82	5.11±0.64	12	0.43	0.67
Right	*x* (cm)	0.42±1.34	0.32±0.98	12	0.25	0.81
	y (cm)	−4.58±0.76	−5.42±0.57	12	−4.81	<0.001
	z (cm)	5.24±1.43	4.89±0.67	12	0.86	0.41

a significant component-by-axis interaction ($F[2,11]=5.5$, $P=0.02$) but no main effect of the component ($F[1,12]=0.4$, $P=0.54$). To further delineate this interaction, we performed paired t-tests for each axis. There was a significant difference in the y-coordinate ($t[12]=-4.8$, $P<0.001$), thus indicating that N100m was located significantly more laterally than P50m. There was no difference in the x-coordinate ($t[12]=0.3$, $P=0.81$) or the z-coordinate ($t[12]=0.9$, $P=0.41$). For the dipole strength, the dipole moments ($\|Q\|$) and directions (Qx, Qy, Qz) of P50m and N100m are shown in Table 3. There were significant Qx and Qz differences between P50m and N100m, thus indicating that the P50m direction is opposite to the N100m. In summary, N100m was located more laterally than P50m for both hemispheres. Fig. 3 shows the source locations of P50m and N100m to the first stimulus of one subject, which are projected onto the appropriate coronal MRI sections. The P50m was located in the HG and the N100m was located in the PT for both hemispheres.

3.4. The dipole source differences between S1 and S1–S2 responses

Nine of the 17 subjects had statistically significant dipoles of P50m, and 11 of the 17 subjects had significant dipoles of N100m in both hemispheres. The x, y, and z-coordinates of the S1 and the S1–S2 responses are shown in Supplement 2. For the left hemisphere, a repeated measures MANOVA demonstrated no main effect of the response (P50m: $F[1,8]=0.1$, $P=0.82$, N100m: $F[1,10]=1.5$, $P=0.24$) with no significant response-by-axis interaction (P50m: $F[2,7]=0.4$, $P=0.68$, N100m: $F[2,9]=1.7$, $P=0.23$). For the right hemisphere, a repeated measures MANOVA demonstrated no main effect of the response (P50m: $F[1,8]=3.5$, $P=0.1$, N100m: $F[1,10]=2.3$, $P=0.16$) with no significant response-by-axis interaction (P50m: $F[2,7]=2.2$, $P=0.18$, N100m: $F[2,9]=0.9$, $P=0.43$).

Table 3
The dipole moments ($\|Q\|$) and directions (Qx, Qy, Qz) of P50m and N100m to the first stimulus for each hemisphere ($n=13$)

		P50m	N100m	df	t	P
Left	$\|Q\|$ (nAm)	11.64±6.37	25.32±6.37			
	Qx (nAm)	4.60±3.15	−13.24±5.53	12	9.04	<0.001
	Qy (nAm)	1.98±5.67	1.79±3.59	12	0.08	0.94
	Qz (nAm)	9.21±7.81	−20.74±5.72	12	12.44	<0.001
Right	$\|Q\|$ (nAm)	13.58±12.97	30.48±12.91			
	Qx (nAm)	3.57±5.02	−14.82±9.22	12	5.62	<0.001
	Qy (nAm)	−1.53±7.23	−2.12±3.81	12	0.25	0.81
	Qz (nAm)	3.43±4.90	−25.65±10.9	12	8.16	<0.001

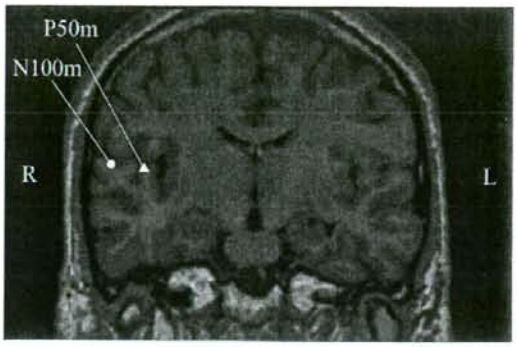

Fig. 3. The locations of the P50m and the P100m sources in the right hemisphere of one subject projected onto the appropriate coronal MRI sections. The triangle signifies the P50m and the circle signifies the N100m. The P50m is located in the Heschl's gyrus and the N100m is located in the Planum Temporale. For this subject, the location of the N100m source is 1.36 cm lateral, 0.18 cm superior and 0.15 cm posterior to the P50m source.

4. Discussion

This study investigated the auditory evoked magnetic fields to voice stimuli using a conditioning–testing paradigm. The major findings of this study were: (1) for RMS both P50m and N100m showed a significant suppression to the second stimulus bilaterally, and the suppression was more significant in N100m; (2) The N100m was located significantly more laterally than the P50m for both hemispheres.

The ability of the brain to suppress incoming irrelevant sensory input is called sensory gating (Freedman et al., 1991). The sensory auditory gating has been found as the P50 suppression in normal subjects (Edgar et al., 2003; Hanlon et al., 2005). Voice recognition represents an evolutionary significant element of social communication. To suppress incoming irrelevant vocal sensory input seems important to solve adaptive problems critical for survival, such as distinguishing friend from foe, familiar from unfamiliar, related from unrelated. It has been reported that deficits of sensory gating cause sensory overload in patients with schizophrenia (Adler et al., 1982; Braff, 1993). Moreover, auditory verbal hallucinations are the most

ɔn symptoms, being reported by approximately 70%
ents with schizophrenia (Sartorius et al., 1986). The
t study indicated a significant suppression of P50m
00m to the second voice stimulus in the bilateral HG
, suggesting that there is the gating effect to vocal
as well as to non-vocal sounds in the human brain.
ture study is thus called for the investigation on the
gating to vocal sounds in patients with schizo-
a. This study also showed that the N100m
ssion was more significant than that for P50m. The
effects of ISI may indicate that the number of
ic chains is larger in the more affected component.
ɔnally, the primary auditory area is mainly located in
, and the auditory association area is located in the
ll et al., 2003); thus it may be reasonable to assume
N100m suppression was more significant than the

N100m peak latency in the current study was
in comparison to several reports on the N100m
l sounds (e.g., Obleser et al., 2003; Tiitinen et al.,
One possible reason for shorter latencies of
ɪ in the current study may be methodological
nces. For example, Obleser et al. (2003) and
n et al. (2005) delivered auditory stimuli
ally and recorded N100m. Yoshiura et al. (1994)
d out that the ipsilateral N100m latency was
d since the ipsilateral N100m was activated
h corpus callosum. Binaurally stimulated
ɪ may be an overlapping activity of the ipsilateral
e contralateral N100m, and thus the N100m
is longer compared to the contralateral N100m
with monaural stimulation.
erms of dipole locations, it was reported that the
ocated anterior to the N100m (Mäkelä et al., 1994;
inen et al., 1998), although statistical significances
nclear in these studies. In the present study, the
ɪ source was localized significantly more laterally
e P50m source. The P50m located anterior and
to the N100m, but these differences did not reach
al significance. Differences in the stimuli (i.e., click,
rst or human voice) used across studies may account
erences in the findings between those studies. In the
study, both P50m and N100m to voice stimulus
cated in STG, while recent fMRI studies reported
lateral STS regions responded to human voice
ely (Belin et al., 2000; Fecteau et al., 2004). In
the single equivalent current dipole indicates the
location of auditory evoked responses. The
ice in the time resolution between MEG and fMRI
be noted.
suppression effect of P50 to the second stimulus
red to as a gating ratio (S2/S1). The gating ratio
of the present study seems smaller compared to previous studies on P50 evoked by click stimuli in normal subjects (Edgar et al., 2003; Hanlon et al., 2005). Chen et al. (1997) reported that the P50 to the human voice stimuli was significantly larger than the P50 to tone burst stimuli and there was no significant difference between stimuli in N100, using a repetitive stimulus paradigm with 2-s ISI. The ISI effect to the P50 elicited by the vocal sound might be smaller compared to the effect to the P50 evoked by non-vocal sounds, perhaps related to a smaller gating effect to vocal sounds.

There are several limitations in this study. First, it should be noted that the present study used shorter IPI compared to previous EEG studies. For EEG, the recovery time of P50 was reported to be around 8 s (Zouridakis and Boutros, 1992), and that of the N100 was reported to be nearly 10 s (Davis et al., 1966). For MEG, Lu et al. (1992) reported that the N100m response was recovered more than 90% with 6-s ISI and the recovery was asymptotic. Second, it is still unclear how methodological differences (e.g. click or voice, durations of stimuli, the number of epochs for averaging) affect MEG waveforms in the conditioning–testing P50 paradigm. Third, we cannot rule out the possibility that all artifacts arose from the head movement of subjects since we used a 37-channel biomagnetometer with a spherical surface covering a circle of 14.4 cm. To reduce artifacts, we registered the locations of the preauricular points and nasion in relation of the biomagnetometer for each session in the present study.

In summary, both P50m and N100m showed a significant suppression to the second stimulus bilaterally, and the N100m was located significantly more laterally than the P50m in both hemispheres. These results are thus considered to demonstrate the presence of sensory gating for the auditory inputs of the human voice in the primary auditory cortex and the auditory association area.

Acknowledgments

This work was supported in part by a grant-in-aid for Scientific Research (C17591218) from the Ministry of Education, Culture, Sports, Science and Technology, Japan (to Dr. Onitsuka). The authors gratefully acknowledge the valuable technical assistance of Mr. Kazumitsu Takahashi and Miss Yuko Somehara.

Appendix A. Supplementary data

Supplementary data associated with this article can be found, in the online version, at doi:10.1016/j.pscychresns.2007.07.002.

References

Adler, L.E., Pachtman, E., Franks, R.D., Pecevich, M., Waldo, M.C., Freedman, R., 1982. Neurophysiological evidence for a defect in neuronal mechanisms involved in sensory gating in schizophrenia. Biological Psychiatry 17, 639–654.

Belin, P., Zatorre, R.J., Lafaille, P., Ahad, P., Pike, B., 2000. Voice-selective areas in human auditory cortex. Nature 403, 309–312.

Boutros, N.N., Trautner, P., Rosburg, T., Korzyukov, O., Grunwald, T., Schaller, C., Elger, C.E., Kurthen, M., 2005. Sensory gating in the human hippocampal and rhinal regions. Clinical Neurophysiology 116, 1967–1974.

Braff, D.L., 1993. Information processing and attention dysfunctions in schizophrenia. Schizophrenia Bulletin 19, 233–259.

Buchwald, J.S., Erwin, R.J., Read, S., Van Lancker, D., Cummings, J.L., 1989. Midlatency auditory evoked responses: differential abnormality of P1 in Alzheimer's disease. Electroencephalography and Clinical Neurophysiology 74, 378–384.

Buchwald, J.S., Erwin, R., Van Lancker, D., Gutherie, D., Schwafel, J., Tanguay, P., 1992. Midlatency auditory evoked responses: P1 abnormalities in adult autistic subjects. Electroencephalography and Clinical Neurophysiology 84, 164–171.

Cacace, A.T., Satya-Murti, S., Wolpaw, J.R., 1990. Human middle-latency auditory evoked potentials: vertex and temporal components. Electroencephalography and Clinical Neurophysiology 77, 6–18.

Chen, C.H., Ninomiya, H., Onitsuka, T., 1997. Influence of reference electrodes, stimulation characteristics and task paradigms on auditory P50. Psychiatry and Clinical Neurosciences 51, 139–143.

Davis, H., Mast, T., Yoshie, N., Zerlin, S., 1966. The slow response of the human cortex to auditory stimuli: recovery process. Electroencephalography and Clinical Neurophysiology 21, 105–113.

Edgar, J.C., Huang, M.X., Weisend, M.P., Sherwood, A., Miller, G.A., Adler, L.E., Cañive, J.M., 2003. Interpreting abnormality: an EEG and MEG study of P50 and the auditory paired-stimulus paradigm. Biological Psychology 65, 1–20.

Erwin, R.J., Buchwald, J.S., 1986. Midlatency auditory evoked responses: differential effects of sleep in the human. Electroencephalography and Clinical Neurophysiology 65, 383–392.

Fecteau, S., Armony, J.L., Joanette, Y., Belin, P., 2004. Is voice processing species-specific in human auditory cortex? An fMRI study. NeuroImage 23, 840–848.

Freedman, R., Adler, L.E., Waldo, M.C., Pachtman, E., Franks, R.D., 1983. Neurophysiological evidence for a detect in inhibitory pathways in schizophrenia: comparison of medicated and drug-free patients. Biological Psychiatry 18, 537–551.

Freedman, R., Waldo, M.C., Bickford-Winner, P., Nagamoto, H., 1991. Elementary neuronal dysfunction in schizophrenia. Schizophrenia Research 4, 233–243.

Godey, B., Schwartz, D., de Graaf, J.B., Chauvel, P., Liégeois-Chauvel, C., 2001. Neuromagnetic source localization of auditory evoked fields and intracerebral evoked potentials: a comparison of data in the same patients. Clinical Neurophysiology 112, 1850–1859.

Grunwald, T., Boutros, N.N., Pezer, N., von Oertzen, J., Fernández, G., Schaller, C., Elger, C.E., 2003. Neuronal substrates of sensory gating within the human brain. Biological Psychiatry 53, 511–519.

Hall, D.A., Hart, H.C., Johnsrude, I.S., 2003. Relationships between human auditory cortical structure and function. Audiology and Neurotology 8, 1–18.

Hanlon, F.M., Miller, G.A., Thoma, R.J., Irwin, J., Jones, A., Moses, S.N., Huang, M., Weisend, M.P., Paulson, K.M., Edgar, J.C., Adler, L.E., Cañive, J.M., 2005. Distinct M50 and M100 auditory gating deficits in schizophrenia. Psychophysiology 42, 417–427.

Huang, M.X., Edgar, J.C., Thoma, R.J., Hanlon, F.M., Moses, S.N., Lee, R.R., Paulson, K.M., Weisend, M.P., Irwin, J.G., Bustillo, J.R., Adler, L.E., Miller, G.A., Canive, J.M., 2003. Predicting EEG responses using MEG sources in superior temporal gyrus reveals source asynchrony in patients with schizophrenia. Clinical Neurophysiology 114, 835–850.

Huizenga, H.M., van Zuijen, T.L., Heslenfeld, D.J., Molenaar, P.C., 2001. Simultaneous MEG and EEG source analysis. Physics in Medicine and Biology 49, 533–539.

Huotilainen, M., Winkler, I., Alho, K., Escera, C., Virtanen, J., Ilmoniemi, R.J., Jääskeläinen, I.P., Pekkonen, E., Näätänen, R., 1998. Combined mapping of human auditory EEG and MEG responses. Electroencephalography and Clinical Neurophysiology 108, 370–379.

Jacobson, P.G., Kraus, N., McGee, J.T., 1997. Hearing as reflected by middle and long latency event-related potentials. In: Alford, B.R., Jerger, J., Jenkins, H.A. (Eds.), Electrophysiologic Evaluation in Otolaryngology. Advances in Oto-Rhino-Laryngology, 53. Karger, Basel, pp. 46–84.

Jessen, F., Kucharski, C., Fries, T., Papassotiropoulos, A., Hoenig, K., Maier, W., Heun, R., 2001. Sensory gating deficit expressed by a disturbed suppression of the P50 event-related potential in patients with Alzheimer's disease. American Journal of Psychiatry 158, 1319–1321.

Kanno, A., Nakasato, N., Maruyama, N., Yoshimoto, T., 2000. Middle and long latency peak sources in auditory evoked magnetic fields for tone bursts in humans. Neuroscience Letters 293, 187–190.

Krause, M., Hoffmann, W.E., Hajos, M., 2003. Auditory sensory gating in hippocampus and reticular thalamic neurons in anesthetized rats. Biological Psychiatry 53, 244–253.

Lee, Y.S., Lueders, H., Dinner, D.S., Lesser, R.P., Hahn, J., Klem, G., 1984. Recording of auditory evoked potentials in man using chronic subdural electrodes. Brain 107, 115–131.

Lütkenhöner, B., Steinsträter, O., 1998. High-precision neuromagnetic study of the functional organization of the human auditory cortex. Audiology and Neurotology 3, 191–213.

Lu, Z.L., Williamson, S.J., Kaufman, L., 1992. Human auditory primary and association cortex have differing lifetimes for activation traces. Brain Research 572, 236–241.

Mäkelä, J.P., Hämäläinen, M., Hari, R., McEvoy, L., 1994. Whole-head mapping of middle-latency auditory evoked magnetic fields. Electroencephalography and Clinical Neurophysiology 92, 414–421.

Neylan, T.C., Fletcher, D.J., Lenoci, M., McCallin, K., Weiss, D.S., Schoenfeld, F.B., Marmar, C.R., Fein, G., 1999. Sensory gating in chronic posttraumatic stress disorder: reduced auditory P50 suppression in combat veterans. Biological Psychiatry 46, 1656–1664.

Ninomiya, H., Onitsuka, T., Chen, C.-H., Kinukawa, N., 1997. Possible overlapping potentials of the auditory P50 in humans: factor analysis of middle latency auditory evoked potentials. Electroencephalography and Clinical Neurophysiology 104, 23–30.

Obleser, J., Elbert, T., Lahiri, A., Eulitz, C., 2003. Cortical representation of vowels reflects acoustic dissimilarity determined by formant frequencies. Cognitive Brain Research 15, 207–213.

Onitsuka, T., Ninomiya, H., Sato, E., Yamamoto, T., Tashiro, N., 2000. The effect of interstimulus intervals and between-block rests on the auditory evoked potential and magnetic field: is the auditory P50 in humans an overlapping potential? Clinical Neurophysiology 111, 237–245.

Onitsuka, T., Shenton, M.E., Salisbury, D.F., Dickey, C.C., Kasai, K., Toner, S.K., Frumin, M., Kikinis, R., Jolesz, F.A., McCarley, R.W., 2004. Middle and inferior temporal gyrus gray matter volume abnormalities in chronic schizophrenia: an MRI study. American Journal of Psychiatry 161, 1603–1611.

Oldfield, R.C., 1971. The assessment and analysis of handedness: The Edinburgh Inventory. Neuropsychologia 9, 97–113.

Pantev, C., Bertrand, O., Eulitz, C., Verkindt, C., Hampson, S., Schuierer, G., Elbert, T., 1995. Specific tonotopic organizations of different areas of the human auditory cortex revealed by simultaneous magnetic and electric recordings. Electroencephalography and Clinical Neurophysiology 94, 24–40.

Sartorius, N., Jablensky, A., Korten, A., Ernberg, G., Anker, M., Cooper, J.E., Day, R., 1986. Early manifestations and first-contact incidence of schizophrenia in different cultures. A preliminary report on the initial evaluation phase of the WHO Collaborative Study on determinants of outcome of severe mental disorders. Psychological Medicine 16, 909–928.

Sarvas, J., 1987. Basic mathematical and electromagnetic concepts of the biomagnetic inverse problem. Physics in Medicine and Biology 32, 11–22.

Spitzer, R.L., Williams, J.B.W., Gibbson, M., First, M., 1990. The Structured Clinical Interview for DSM-III-R (SCID-NP)-Non-Patient Edition. American Psychiatric Association, Washington, DC.

Tiitinen, H., Mäkelä, A.M., Mäkinen, V., May, P.J., Alku, P., 2005. Disentangling the effects of phonation and articulation: hemispheric asymmetries in the auditory N1m response of the human brain. BMC Neuroscience 6, 62.

Yamamoto, T., Williamson, S.J., Kaufman, L., Nicholson, C., Llinás, R., 1988. Magnetic localization of neuronal activity in the human brain. Proceedings of the National Academy of Sciences of the United States of America 85, 8732–8736.

Yoshiura, T., Ueno, S., Iramina, K., Masuda, K., 1994. Effects of stimulation side on human middle latency auditory evoked magnetic fields. Neuroscience Letters 172, 159–162.

Yoshiura, T., Ueno, S., Iramina, K., Masuda, K., 1995. Source localization of middle latency auditory evoked magnetic fields. Brain Research 703, 139–144.

Zouridakis, G., Boutros, N.N., 1992. Stimulus parameter effects on the P50 evoked response. Biological Psychiatry 32, 839–841.